

The very local Hubble flow: Simulating transition from chaos to order

A. D. Chernin^{1,2}, I. D. Karachentsev³, M. J. Valtonen^{1,4}, V. P. Dolgachev², L. M. Domozhilova², and D. I. Makarov^{3,5}

¹ Tuorla Observatory, Turku University, Piikkiö, 21 500, Finland

² Sternberg Astronomical Institute, Moscow University, Moscow, 119899, Russia

³ Special Astrophysical Observatory, Nizhnii Arkhys, 369167, Russia

⁴ University of West Indies, Trinidad and Tobago

⁵ Isaac Newton Institute of Chile, SAO Branch, Russia

Received / Accepted

Abstract. The physical nature of the very local (≤ 3 Mpc) Hubble flow is studied on the basis of the recent high precision observations in the Local Volume. A model including both analytical treatment and computer simulations describes the flow dynamical evolution from a chaotic Little Bang initial state to the present-day state of a quasi-regular expansion. The two major observational parameters of the flow, which are the rate of expansion and the velocity dispersion, find a clear qualitative and quantitative explanation in the model.

Key words. galaxies: Local Group

1. Introduction

It has long been taken for granted in theoretical cosmology that the notion of the cosmological expansion is applicable to only very large spatial distances, and that only at the scale of great clusters of galaxies, the markers that participate in the cosmological expansion can be found. A reason for this comes from the fact that the expansion with the linear velocity-distance relation is directly associated with the uniformity of the Universe, in the Friedmann standard cosmological theory. Since the matter distribution is uniform only at the spatial scales larger than 100–300 Mpc, the cosmological expansion is treated as a phenomenon of the largest observed scales. However, in drastic contradiction with this view, the phenomenon was originally discovered by Hubble in the Local Volume within 20 Mpc distance from us. The Local Volume is deep inside the cosmic cell of matter uniformity, and observations reveal a significant non-uniformity in the spatial

distribution of galaxies there. How may the regular linear velocity field be compatible with the observed spatial non-uniformity of the galaxy distribution in the Local Volume? How might the cosmological phenomenon be discovered so closely to us?

The questions were clearly stated by Sandage (1986; see also Sandage et al. 1972). In a recent paper, Sandage (1999) concludes that an “explanation of why the local expansion field is so noiseless remains a mystery”. It is also puzzling that the local rate of expansion is similar to the global one, if not exactly the same, within 10–15 percent accuracy (Sandage 1999). This is the Hubble-Sandage paradox described in more detail in our earlier paper (Chernin, Karachentsev, Valtonen et al. 2004 — hereafter Paper I).

A possible solution to the Hubble-Sandage paradox has been suggested by Chernin, Teerikorpi and Baryshev (2000) soon after the discovery of cosmic vacuum (dark energy or the cosmological constant) in distant supernova Ia observations (Riess et al. 1998, Perlmutter et al. 1999). It has been recognized (Chernin 2001, Baryshev, Chernin, Teerikorpi 2001) that cosmic vacuum with its perfectly uniform density makes the Universe effectively uniform at various spatial scales, both large and relatively small, where cosmic vacuum dominates by density over dark matter and baryons. The dynamical effect of cosmic vacuum is enhanced by the fact that the effective gravitating density of vacuum is $\rho_V + 3p_V = -2\rho_V$, where $p_V = -\rho_V$ is the vacuum pressure. In the Local Volume, vacuum dominates by force at the distances larger than $R_V \simeq 1.5\text{--}2$ Mpc from the barycenter of the Local Group. On the ‘zero-gravity surface’ of the size $\simeq R_V$, the gravity of the Local Group dark matter and baryons is balanced by the antigravity of vacuum. Observations show that these are just the distances from which the observed Hubble flow takes start.

These considerations suggest that cosmic vacuum may control the dynamics of the observed Universe at both global spatial scales approaching the observation horizon and local scales deep inside the cell of matter uniformity. Because of this, the cosmological expansion may be not only a global phenomenon, but also a local one. On all the spatial scales where vacuum dominates, the expansion rate may be exactly or nearly the same, since the rate (measured by the Hubble factor) is mainly determined by one and the same physical agent which is vacuum with its perfectly uniform density (Karachentsev, Chernin, Teerikorpi 2003).

As Sandage and his colleagues comment this idea, “...the total force field is nearly homogeneous (smooth) due to the dominance of an all pervasive cosmological constant, diluting any lumpy gravity field of the clustered matter...” (Thim et al. 2003).

Cosmological N-body LambdaCDM simulations performed by Macciò et al. (2005) are reported to confirm both qualitative and quantitative conclusions of our papers mentioned above. A theory treatment by Leong and Saslaw (2004) within the framework of many-body gravitational clustering shows that the observed small departures from the regular Hubble flow beyond the Local Group are highly probable. They also find that

low mass groups, like the Local Group, dominate, and the Hubble flow is not significantly disturbed around them. Important observed features of the local expansion flow are discussed by Whiting (2003), Axenides and Perivolaropoulos (2002).

The nearest to us part of the expansion flow, the very local (< 3 Mpc) Hubble flow (VLHF), is obviously of a special interest: it is the area where the expansion takes its origin. In Paper I, we presented most recent data on the VLHF kinematics including original distance measurements made mostly with the *Hubble Space Telescope* (Karachentsev et al. 2000, 2002, 2003). The data display the VLHF as a well organized outflow with the linear velocity-distance relation. Its expansion rate is $72 \pm 15 \text{ km s}^{-1} \text{ Mpc}^{-1}$ and the one-dimension random mean motion is about 30 km s^{-1} .

As a first step in the search for the VLHF physical nature, we performed a set of computer simulations to reconstruct the dynamical history of the flow. We found (Paper I) that the evolution of the VLHF might begin at the epoch of the Local Group formation some 12.5 Gyr ago. At that time, the VLHF galaxies, together with the forming major galaxies of the group and a variety of subgalactic units, participated in violent nonlinear dynamics with multiple collisions and merging. This violent initial state is essentially similar to the Little Bang model (Byrd et al. 1994) and the concept of the early Local Group described by van den Bergh (2003). We demonstrated that the VLHF might be formed by relatively small units that survived accretion by the major galaxies and managed to escape from the gravitational potential well of the Local Group to the area outside the local zero-gravity surface. A typical VLHF member galaxy gained escape velocity from the non-stationary gravity field of the forming group and a velocity larger than some 200 km s^{-1} enabled it to reach the vacuum-dominated area where they gained additional acceleration from cosmic vacuum.

According to the results of Paper I, the VLHF is not a slightly disturbed initial cosmological flow with the linear velocity law existed from the ‘very beginning’. On the contrary, the observed members of the VLHF underwent strong nonlinear interactions with the major galaxies of the Local Group before they formed the quasi-regular flow outside the zero-gravity surface. Their initially chaotic motions became quasi-regular under the combine action of the quasi-static and quasi-spherically symmetric gravitational potential of the Local Group outside the local zero-gravity surface and the vacuum which controlled the flow further dynamics there.

In the present paper, we develop the systematic studies of the VLHF along the line traced in Paper I. We focus now on the physics which controls the flow transition from the initial chaos to the present-day order. Two key aspects of the problem are the dynamical cooling of the expansion flow outside the local zero-gravity surface, which is studied analytically in Sec.2, and the structure of the chaotic motions inside this surface, which is a subject of computer simulations presented in Sec.3. A discussion of the results is given and the major conclusions are summarized in Sec.4.

2. Vacuum cooling

Following the results of Paper I, we assume that the VLHF takes its origin in the Little Bang developed inside the zero-gravity (ZG) surface. Each VLHF galaxy participates in the violent nonlinear dynamics of a many-body system of primeval galaxies and gaseous subgalactic clumps moving in the non-stationary gravitational potential of the early Local Group some 12.5 Gyrs. When a galaxy crosses the ZG surface, it enters the area where the gravitational potential is nearly spherically symmetric and almost static. The former is clearly indicated by the shape of the local ZG surface which is nearly spherical and only slightly changes approaching in shape to the perfect static sphere, asymptotically (Figs.5–8 below; see also Dolgachev et al. 2003, 2004 for more details). A typical trajectory of the small body (a dwarf galaxy) is nearly radial, in such a potential, as computer simulations show (see Sec.3). Therefore the first stage of the transition from chaos to order occurs within the ZG surface, when an initially chaotic outflow of escaping galaxies becomes more or less radial reaching the sphere. But this nearly radial flow remains rather ‘hot’: its radial velocity dispersion is still high at the surface. The outflow cooling is the second stage of the transition process.

In this section, we focus on the second stage of the transition process. Due to the nearly radial symmetry of the outflow, a simple analytical treatment is possible for this stage (the first stage is studied in the next section with the use of computer simulations).

Let us follow the motion of a small body (a test particle) outside the ZG surface along a radial trajectory. We will consider the particle a ‘typical’ member of the VLHF. Neglecting in the first approximation any (small) deviations of the ‘matter part’ of gravitational potential from the spherical shape, we may describe the trajectory by the Newtonian equation of motion in the form:

$$\ddot{r}(t) = -GM/r^2 + r/A_V^2, \quad r \geq R_V. \quad (1)$$

The gravity of matter and the antigravity of vacuum are represented in the right-hand side of the equation by the terms of the opposite signs. Here r is the distance of the body to the Local Group barycenter, $M = 2 \times 10^{12} M_\odot$ is the mass of the group, including both dark matter and baryons. The value $A_V = (\frac{8\pi G}{3} \rho_V)^{-1/2} \simeq 1.5 \times 10^{28}$ cm is the vacuum characteristic length (the Friedmann integral for vacuum — see Chernin 2001), and $\rho_V = 7 \times 10^{-30}$ g cm⁻³ is the vacuum density. (Hereafter the speed of light $c = 1$ in the formulas.)

The ZG surface at which $\ddot{r} = 0$ is a sphere of the radius

$$R_V = (GMA_V^2)^{1/3} \simeq 1.5 \text{ Mpc}. \quad (2)$$

The mathematical structure of Eq.1 is similar to the structure of the Friedmann cosmological equation for the global expansion scale factor $R(t)$:

$$\ddot{R}(t, \chi) = -GM(\chi)/R^2 + R/A_V^2, \quad (3)$$

where $M(\chi) = \text{Const}(t)$ is the mass of non-relativistic dark matter and baryons within the sphere of the Lagrangian radius $R(\chi, t)$, and χ is the Lagrangian coordinate of the body. The difference of Eq.3 from Eq.1 is in the dependence of M on the Lagrangian coordinate. According to Eq.1, each body moves in the potential of the same gravitational mass, while Eq.3 indicates that the mass is different for different χ , i.e. different particles. The ‘vacuum part’ of the gravitational potential and force is the same in both Eq.1 and Eq.3. Asymptotically, when r and R go to infinity, vacuum dominates entirely, and the difference between the equations vanishes: they coincide completely. In this limit, both equations give the same velocity-distance law $\dot{r} = r/A_V$ and $\dot{R} = R/A_V$. Then the expansion rate, the Hubble factor $H_V = 1/A_V$ is a constant in both cases. This asymptotic similarity of the equations is significant: it indicates that the motion of the particle we follow tends asymptotically to the cosmological regime. In conventional units, $H_V = 1/A_V \simeq 60 \text{ km s}^{-1} \text{ Mpc}^{-1}$. This value is in agreement with the observational data; according to (Karachentsev et al. 2002, 2003), the expansion rate for the VLHF is $72 \pm 15 \text{ km s}^{-1} \text{ Mpc}^{-1}$ (see Sec.1).

A close relation to cosmology is seen not only in the vacuum part of the potential, but also in its matter part. Indeed, the total mass of the Local Group (which is mostly dark matter mass in the halos of the two major galaxies of the group) together with the mass of all the bodies of the VLHF are collected from the initially uniform cosmological matter distribution. An ‘unperturbed’ cosmological volume containing the non-relativistic mass M has the present-day radius

$$R_M = \left[M / \left(\frac{4\pi}{3} \rho_M \right) \right]^{1/3} \simeq 2 \text{ Mpc}. \quad (4)$$

Here $\rho_M = \rho_D + \rho_B \simeq 3 \times 10^{-30} \text{ g cm}^{-3}$ is the sum of the dark matter density and the baryonic density at present. A near coincidence of the values R_M and R_V is obviously a result of the near coincidence of the mean dark matter density and the vacuum density in the present-day state of the Universe.

This means that the analytical model described by Eq.1 has a direct connection to cosmology, since its both parameters, M and A_V , have a clear cosmological meaning: cosmology parameters are imprinted in the dynamical background on which the local expansion flow develops.

The first integral of Eq.1 expresses, as usual, the mechanical energy conservation:

$$\frac{1}{2} \dot{r}^2 = GM/r + \frac{1}{2} (r/A_V)^2 + E, \quad (5)$$

where $E = \text{Const}$ is different, generally, for different particles. When the trajectory crosses the ZG surface and $r = R_V$, one has from Eq.5:

$$\dot{r}^2 = 3(R_V/A_V)^2 + 2E, \quad r = R_V. \quad (6)$$

Let us introduce a ‘random’ velocity v as a difference between the velocity \dot{r} and a ‘regular’ (asymptotic) velocity r/A_V . Then the random velocity v at $r = R_V$,

$$v_1 = (R_V/A_V) \left[(3 + 2EA_V^2/R_V^2)^{1/2} - 1 \right]. \quad (7)$$

As the trajectory reaches the distance r outside the ZG surface, the random velocity $v(r)$ is given (for an arbitrary E) by the relation:

$$v(r) = (R_V/A_V) \left[(r^2/R_V^2 - 2 + 2R_V/r + 2v_1A_V/R_V + v_1^2A_V^2/R_V^2)^{1/2} - r/R_V \right]. \quad (8)$$

A comparison of $v(r)$ with v_1 enables to find how the random velocity decreases along the particle trajectory. For this goal, we may introduce the ‘vacuum cooling factor’, $q_V \equiv v_1/v$ which measures the efficiency of the random velocity suppression due to vacuum:

$$q_V = (v_1A_V/R_V) \left[(r^2/R_V^2 + 2 + 2R_V/r + 2v_1A_V/R_V + v_1^2A_V^2/R_V^2)^{1/2} - r/R_V \right]^{-1}. \quad (9)$$

In the simplest case when the total energy is zero, $E = 0$, the velocity $v_1 = (\sqrt{3} - 1)R_V/A_V$, and we have from Eq.8:

$$v(r) = (R_V/A_V) \left[(r^2/R_V^2 + 2R_V/r)^{1/2} - r/R_V \right]. \quad (10)$$

Then the vacuum cooling factor in the parabolic expansion flow

$$q_V(r) = v_1/v(r) = (\sqrt{3} - 1) \left[(r^2/R_V^2 + 2)^{1/2} - r/R_V \right]^{-1}. \quad (11)$$

We may see from Eqs.7,11 that the random velocity is diminished by factor $\simeq 3$ — from $\simeq 70$ to $\simeq 20$ km s $^{-1}$ — during the time when the body covers the path from $r = R_V$ to the VLHF upper spatial limit $r \simeq 2R_V \simeq 3$ Mpc. The resulting random velocity is in agreement with the observational value of 30 km s $^{-1}$ (see Karachentsev et al. 2002, 2003 and Sec.1). When the same body reaches, say, distances 4 or 6 R_V , the cooling factor increases to $q_V = 12$ and $q_V = 56$, correspondingly.

If the random velocity $v(r)$ is small compared to the regular velocity r/A_V and $E = 0$, one finds from Eq.5 in the linear approximation:

$$v \simeq R_V^3/(A_V r^2) \propto r^{-2}. \quad (12)$$

Recall that the cosmological adiabatic cooling is described by the relation $v \propto R^{-1}$. We may conclude that the vacuum cooling of the local Hubble flow acts much more effectively than the adiabatic cooling.

The second integral of Eq.5 (for $E = 0$) has a well-known exact solution: $r \propto \sinh[\frac{3}{2}t/A_V]^{2/3}$. Then the law of vacuum cooling in the linear approximation takes the form:

$$q_V \propto \sinh[\frac{3}{2}t/A_V]^{4/3}. \quad (13)$$

It is interesting — for comparison — to follow the dynamics of the same expansion flow, but in the absence of cosmic vacuum. With the same statement of the problem as

above, but with $\rho_V = 0$ and $E > 0$, we would have an asymptotic (as r goes to infinity) motion which is an inertial one: $\dot{r} = (2E)^{1/2}$. This is also a Hubble-type motion with the linear velocity-distance relation: $\dot{r} = r/t$, where the expansion rate, $H_E = 1/t$, depends on time. This suggests that the flow may be cooled without vacuum as well (see also Sec.3); but the cooling efficiency is much lower in the absence of vacuum. Indeed, taking r/t as a regular motion velocity, we may introduce the random velocity v by the relation $\dot{r} = r/t + v$. Then from Eq.5 (without the vacuum term) we find:

$$v = (2E)^{1/2} \left[\left(1 + \frac{GM}{2Er} \right)^{1/2} - 1 \right]. \quad (14)$$

In the linear approximation for $v/(2E)^{1/2} < 1$, this leads to the adiabatic relation $v \propto r^{-1}$. As a result, the cooling factor in the absence of vacuum, $q_E \propto r$, is significantly smaller than the vacuum cooling factor q_V of Eqs.9, 11, 13.

Thus, vacuum cooling reveals a high efficiency resulting in the rapid suppression of the random velocity in the outflow outside the local ZG surface. The quantitative similarity of the resulting VLHF parameters is due to the fact that the outflow dynamics develops on the dynamical background with the cosmology-related parameters.

3. Computer simulations: from Little Bang to VLHF

The VLHF evolution inside the local ZG surface cannot be described in any simple analytical model. It is controlled by complex nonlinear dynamics which may be followed — but only to some extent — with computer simulations. The Little Bang model (Byrd et al. 1994) and the picture of the early Local Group (van den Bergh 2003) provide important insights to this dynamics. Basing on this, we developed a simplified approach in which the free fall of the two major galaxies of the Local Group on the cosmic vacuum background plays a central part. This is a ‘Little Bang Minimal Model’ (LBMM) which takes into account that 1) the mass of the Local Group (LG) is mostly dark mass and it strongly concentrates (Karachentsev et al. 2002) to the two major galaxies of the group; 2) the dark matter halos of the Milky Way (MW) and the Andromeda Galaxy (AG) are nearly spherical; 3) the relative MW-AG motion is directed along the line of the centers of the galaxies, in accordance with the classic treatment (Kahn and Woltjer 1959); 4) the LG is embedded in cosmic vacuum which is represented by perfect medium with a uniform constant energy density.

The parameters of the model are the total mass of MW $1 \times 10^{12} M_\odot$, the total mass of AG $1.5 \times 10^{12} M_\odot$ and the vacuum density $\rho_V = 7 \times 10^{-30} \text{ g/cm}^3$ (so the total mass of the Local Group is somewhat larger here than in Sec.2). With the present separation 0.7 Mpc and the present relative velocity -120 km s^{-1} , the two major galaxies of the LG started their motion toward each other 12.5 Gyr ago, in the LBMM. Like in the section above, the motions of the VLHF dwarf galaxies inside are considered as test particle motions, so that the problem under consideration is reduced to the three-body restricted

problem. Despite its obvious simplicity, the LBMM demonstrates a variety of dynamical patterns that might play, as we demonstrate below, the central part in the origin and evolution of the VLHF.

The initial (12.5 Gyr ago) conditions for the particle trajectories are chosen in the three-dimensional axially symmetrical phase space of positions and radial velocities of the LBMM. The phase space is scanned uniformly in the radial velocity range from -500 to 500 km s^{-1} and the radial distance range from 0.15 to 0.80 Mpc . Both velocities and distances are related to the LG center-of-mass. Two sets of 420 trajectories each are integrated — one in the model with cosmic vacuum and the other in the model with no vacuum, for comparison. According to the results of the integration, 397 and 409 trajectories of the first and the second sets, respectively, are found in the VLHF distance interval (from 1.5 to 3 Mpc) at the present-day epoch. These two subsets serve as the banks of trajectories for the further statistical analysis. To simulate the observed sample of the 22 VLHF galaxies (its description see in Paper I), we used model samples of 22 trajectories each selected randomly from each of the two subsets of trajectories.

Table 1 shows 10 such simulation samples of trajectories in the model with the observed vacuum density. Each sample is characterized by the linear regression factor (calculated with the least square method) and the corresponding linear velocity dispersion. The both are calculated for the present and the initial states of the sample. The present regression factor (the first line in Table 1) gives the expansion time rate which may be compared with the observed VLHF Hubble factor. The present velocity dispersion (the second line) is to be compared with the observed velocity dispersion. The initial regression factor (the third line) and the initial velocity dispersion (the fourth line) give a quantitative measure of the chaotic state of the flow 12.5 Gyr ago.

Table 1

1	2	3	4	5	6	7	8	9	10
86.30	98.85	69.41	145.20	91.95	123.08	104.24	100.82	115.05	74.91
30.29	31.46	32.53	27.16	36.81	31.29	20.93	29.52	36.80	34.66
-225.96	-109.43	-74.81	311.66	-121.96	278.96	-130.24	-117.33	-12.17	-152.04
185.13	198.54	182.22	193.88	193.20	187.50	197.39	171.62	178.48	198.94

Table 2

1	2	3	4	5	6	7	8	9	10
74.93	60.55	86.66	85.87	105.07	97.17	87.03	56.57	78.80	46.80
36.99	37.50	29.59	39.59	37.15	32.15	34.98	36.91	34.22	33.49
−19.39	153.65	123.25	301.90	362.22	−3.34	−173.21	−25.99	−331.72	80.69
198.97	185.39	198.75	192.67	174.79	203.86	209.54	212.12	201.32	203.77

Table 3

1	$Vr \pm 50$	$Vr \pm 100$	0 ± 100
86.30	84.47	78.02	27.56
30.29	28.45	24.60	65.27

Let us look, for instance, at the figures of Sample 1 in Table 1. The present-day state of the sample imitates well the observed VLHF. Indeed, the regression factor is $86 \text{ km s}^{-1} \text{ Mpc}^{-1}$ which is within the one-sigma interval of the observed value of the local Hubble parameter, $H_L = 72 \pm 15 \text{ km s}^{-1} \text{ Mpc}^{-1}$ (Karachentsev et al. 2002, 2003). The flow is quiet and cool: its velocity dispersion is 30 km s^{-1} which coincides exactly with the observed value. The present-day Hubble diagram for Sample 1 is showed in Fig.1; it looks very similar to the the real Hubble diagram for the VLHF (Karachentsev 2001).

The initial state of the sample differs drastically from the present one. Indeed, the initial regression factor is negative for Sample 1 of Table 1; it means that the flow was contracting, not expanding, 12.5 Gyr ago. The corresponding initial velocity dispersion is rather high, near 200 km s^{-1} . Both figures show clearly that the initial state was highly chaotic and had nothing in common with an imaginary regular (or slightly disturbed) cosmological expansion flow on similar spatial scales some 12.5 Gyr ago.

Looking at the other samples of Table 1, we may see that, at the present-day state of the model samples, they are characterized by the regression factors which spread from 74 to $123 \text{ km s}^{-1} \text{ Mpc}^{-1}$, and by the velocity dispersion within a rather narrow interval $27\text{--}37 \text{ km s}^{-1}$. Their initial states are highly chaotic and may be both contracting or expanding. The initial velocity dispersion is near 200 km s^{-1} for all the samples.

Table 1 and Fig.1 demonstrate that the LBMM phase space may host highly chaotic sets of the initial states, and they give rise eventually quasi-regular outflows with the linear velocity-distance relation and the expansion rate close to the observed one. It is

most remarkable that the present velocity dispersion values are confined within a rather narrow interval, between 20 and 40 km s⁻¹.

The internal dynamical structure of the samples of Table 1 in the present-day state is illustrated by histograms of Fig.2. The histograms give the distributions of the ‘individual expansion rates’ which are velocity-distance ratios for the members of a sample. We may see that, in a typical case, there is a dominant group of trajectories which determines the overall statistical characteristics of the samples.

Table 2 shows the data for the simulation samples in the model without vacuum. We may see that the major trend in the dynamical evolution is the same: this is a transformation of a flow from chaos to order. The similarity with the vacuum model in this respect is not quite unexpected, in view of the analysis of Sec.2. Indeed, the existence of a regular asymptotic states with the linear velocity-distance relation is rather universal, as is seen from both analytical treatment and computer simulations described by Figs.1,2. The vacuum effect enhances the trend to order essentially, and this reveals clearer at larger distances in the local expansion flows. On the modest distances of the VLHF, the quantitative difference between the two models is not too significant. One may only notice somewhat lower values of the final regression factor, between 47 and 105 km s⁻¹ Mpc⁻¹, and somewhat larger values of the velocity dispersion in a narrow range from 32 to 38 km s⁻¹, in the models without vacuum.

Taking Sample 1 of Table 1 as a typical one, we show its 22 trajectories in the plane of symmetry of the Local Group — see Fig.3. The local ZG surface is showed in the section of this plane; both initial (dash line) and present day (solid line) shape of the surface are given in the figure. It is seen that the surface is rather circular and change with time only very slightly for the last 12.5 Gyr. The most of the trajectories intersect the ZG surface along nearly radial directions. The geometry of most of the trajectories is rather simple: they are very close to straight lines, outside the ZG surface (this fact was used in the analytical treatment of Sec.2). At least in part, such a geometry is due to the initial conditions at which the velocities had only a radial component.

A possible effect of initial non-radial velocities was especially studied for same Sample 1. For this goal, the dimensionality of the LBMM initial phase space was extended from 3 to 4, to include transverse velocities. Fig.4 shows the trajectories of the same galaxies, but with the additional transverse velocity which is initially ± 50 km s⁻¹ for the members of the sample. Fig.5 illustrates the effect of initial transverse velocities of ± 100 km s⁻¹. Finally, Fig.6 shows (unrealistic) trajectories with zero initial radial velocity and with initial transverse velocities of ± 100 km s⁻¹; this is actually a case of an initial rapid rotation of the masses of the ensemble around the LG barycenter, and most of the trajectories prove to be kept within the local ZG surface. With the exception of the unrealistic example of Fig.6, the initial transverse velocities do not alter significantly the simple nearly straight-line geometry of typical trajectories outside the ZG surface.

In addition, Table 3 gives quantitative characteristics of the effect of the transverse velocities — the present expansion rate (the first line) and velocity dispersion. A comparison with the data for Sample 1 of Table 1 shows that the realistic initial transverse velocities (columns 2,3) are compatible with the major trend of the sample evolution. They do not change practically the statistical characteristics of the outflow present-day state. Indeed, with the transverse velocities ± 50 and ± 100 km s⁻¹, the expansion rate decreases slightly (from 86 to 85 and 78 km s⁻¹, correspondingly) keeping within the same one-sigma interval of the observation figure. The velocity dispersion does not change significantly either. Only in the unrealistic case of zero initial radial velocities (column 4), the figures turn out to be considerably different.

Thus, almost a thousand model trajectories have enabled us to simulate the origin of the VLHF and its dynamical evolution within the zero-gravity surface and out of it. In agreement with the analytic considerations of Sec.2, the simulations prove the real possibility of the VLHF evolution from the Little Bang chaos to the order and regularity at present.

4. Discussion and conclusions

The recent high precision mapping of the local velocity field and high accuracy distance measurements in the Local Volume (Karachentsev et al. 2000, 2001, 2002, 2003, 2004; Karachentsev and Makarov 2000; Ekholm et al. 2001; Davidge and van den Bergh 2001; Teerikorpi and Paturel 2002; Thim et al. 2003; Paturel and Teerikorpi 2004, Reindl et al. 2005) have given a clear picture of the nearest Universe. The results have reliably confirmed the earlier conclusions by Sandage et al. (1972) and Sandage (1986, 1999): there is a regular local (within 20 Mpc distance) Hubble flow of expansion deep inside the cell of matter uniformity; it has the expansion rate near the global Hubble constant and the remarkably low velocity dispersion. An understanding of the physical nature of the local Hubble flow has come with the discovery of cosmic vacuum (or the cosmological constant): vacuum with its perfectly uniform dominant density provides dynamical conditions for a regular flow in the highly non-uniform matter distribution (Chernin et al. 2000, Chernin 2001, Baryshev et al. 2001, Karachentsev et al. 2003).

Our further attempts along this line of studies are focused on the very local (≤ 3 Mpc) area of the flow where it takes start. It has led us to a conclusion (Paper I) that the very local Hubble flow was generated in the Little Bang due to the chaotic dynamics of the forming Local Group. In the present paper, we studied the physics of the transition from the initial chaotic state of the flow to its presently observed regular state.

The transition from chaos to order is known in various areas of natural (and also social) sciences, but poorly understood yet. It has been found in fundamental nonlinear physics and, in particular, in the theory of turbulence, that a high degree of complexity

is characteristic for this process. Remarkably enough, in the case of the very local Hubble flow (VLHF), the nonlinear phenomena we face may be clarified and treated in a fairly simple way. The Little Bang Minimal Model (LBMM) enables us to describe the problem in an explicit form and find both qualitative and quantitative solutions to it. The solution we obtain proves to be in a good agreement with the high precision observations mentioned above.

Indeed, the nature of the VLHF initial chaos is not too puzzling in our model. It is, first, due to random choice of the initial states of the VLHF members in the phase space of the Local Group embedded in cosmic vacuum. Second, it is due to the nonlinear three-body dynamics of gravitational scattering of a test mass on a non-stationary massive binary system. The gravitational scattering is a complex process; the dynamical instability is the major physical factor that controls it and introduces the Poincaré-type chaos to the system (see, for a reviews Valtonen and Mikkola 1991, Chernin and Valtonen 1998). But numerical solutions and computer simulations of this process may easily be performed: under the particular conditions described by the LBMM, the simulations are reduced to the standard integration of the three-body restricted problem (Sec.3). The only new feature is the vacuum background on which the process develops.

It turns out that, when the test body escapes from the two-body gravitational potential, the dynamical instability gradually ceases with the distance from the system barycenter, and the third body occurs in the potential which becomes more and more centrally symmetrical. This is clearly seen from the computed geometry of the local zero-gravity (ZG) surface. In fact, the escaped body is affected mainly by a simple nearly centrally-symmetrical potential. This potential is practically static: its evolution is very slow, as is seen from the comparison of the initial and final shape and size of the zero-gravity surface (Figs.3–6). Under such conditions, the motion of the scattered body becomes more and more regular. In a sample of bodies imitating the VLHF, it leads to a picture of a flow which acquires the linear velocity-distance relation, and the deviations from this relation decrease with time.

Cosmic vacuum which starts to dominate dynamically outside the ZG surface of the Local Group introduces additional stability and regularity to the sample evolution. First, it produces perfectly symmetrical and static major contribution to the gravitational potential. Second, it accelerates the escaped bodies and so leads to larger distances from the system barycenter for the life time of the system. At large distances from the center, where vacuum dominates completely, the velocity-distance ratio tends to a constant value $H_V \simeq 60 \text{ km s}^{-1} \text{ Mpc}^{-1}$, independently of the initial conditions.

Our computer simulations enable us also to find that, at the small and modest distances characteristic for the VLHF galaxies, the dynamical tendency introduced by cosmic vacuum is quite recognizable, while it is not too significant quantitatively. But at

larger distances like 4–8 Mpc in the local Hubble flow, the dynamical effect of vacuum is most important both qualitatively and quantitatively.

Outside the ZG surface, the motions of the VLHF members can also be studied with the use of exact analytical solutions. The solutions give a description of the flow evolution to the quasi-regular final state. The solutions show that the flow reach asymptotically a regular structure with the linear velocity-distance relation. This is found in the solutions with vacuum and even in the solutions with no vacuum (Sec.2). In both cases, the flow motion has an asymptotic regime, which is described by a simple, stable and self-similar solution. In accordance with a general result of nonlinear mechanics, this solution is a dynamical attractor for wide classes of more complex solutions.

However the asymptotic regular regime is reached with different efficiency, in the two cases under consideration. The most efficient evolution from chaos to order proceeds in the solution with cosmic vacuum. A quantitative measure of the efficiency of this evolution is the ‘vacuum cooling factor’ introduced and estimated in Sec.2. It describes the vacuum contribution to the VLHF evolution and demonstrates — together with the computer simulations — that cosmic vacuum provides the most effective mechanism of the flow transition from chaos to order, especially at larger distances in the local Hubble flow. It is cosmic vacuum that makes the whole local flow of expansion — from the ZG surface to its maximal spatial scales — a self-consistent regular cosmological phenomenon.

Acknowledgements. We thank Yu. Efremov, G. Byrd, A. Silbergleit, A. Cherepashchuk and A. Zasov for discussions. DIM and ADC acknowledge support from INTAS grant 03–55–1754 and the Russian Foundation for Basic Research grant 03–02–16288. DIM is thankful to the Russian Science Support Foundation for support.

References

- Baryshev Yu.V., Chernin A.D., Teerikorpi P. 2001, *A&A*, 378, 729
- Byrd G., Valtonen M., McCall M., Innanen K. 1994, *AJ* 107, 2055
- Chernin A.D. 2001, *Physics-Uspekhi*, 44, 1099
- Chernin A.D., Valtonen M.J., 1998, *New AR*, 42, 41
- Chernin A.D., Teerikorpi P., Baryshev Yu.V. 2000, [*astro-ph/0012021*] *Adv. Space Res.*, 31, 459, 2003
- Chernin A.D., Karachentsev I.D., Valtonen M.J., Dolgachev V.P., Domozhilova L.M., Makarov D.I. 2004, *A&A* 415, 19 (Paper I)
- Dolgachev V.P., Domozhilova L.M., Chernin A.D. 2003, *Astr.Rep.* 47, 728
- Dolgachev V.P., Domozhilova L.M., Chernin A.D. 2004, *Astr.Rep.* 48, 787
- Giovanelli R., Dale D., Haynes M., Hardy E., Campusano L. 1999, *ApJ*, **525**, 25
- Kahn F.D., Woltjer L. 1959, *ApJ*, 130, 705
- Karachentsev I.D., Chernin A.D., Teerikorpi P. 2003, [*astro-ph/0304250*] *Astrophysics*
- Karachentsev I.D., Sharina M.E., Grebel E.K., et al. 2000, *ApJ*, 542, 128
- Karachentsev I.D., Sharina M.E., Dolphin A.E., et al. 2002, *A&A*, 385, 21

- Karachentsev I.D., Sharina M.E., Makarov D.I., et al. 2002, A&A, 389, 812
- Karachentsev I.D., Makarov D.I., Sharina M.E., et al. 2003, A&A, 398, 479
- Leong B., Saslaw W.C. 2004, ApJ, 608, 636
- Maccio ò A.V., Governato F., Horellow C. 2005 MNRAS.tmp..353M
- Perlmutter S., Aldering G., Goldhaber G., et al. 1999, ApJ, 517, 565
- Reindl B., Tamman G.A., Sandage A., Saha A. 2005, AJ 624, 532
- Riess A.G., Filippenko A.V., Challis P., et al. 1998, AJ 116, 1009
- Sandage A. 1986, ApJ, 307, 1
- Sandage A. 1999, ApJ, 527, 479
- Sandage A., Tammann G., Hardy E. 1972, ApJ, 172, 253
- Teerikorpi P. 1997, ARA&A, 35, 101
- Thim F., Tammann G., Saha A., Dolphin A., Sandage A., Tolstoy E., Labhardt L. 2003, ApJ, 590, 256
- Valtonen M.J., Mikkola S., AR&A, 29, 9
- van den Bergh S. 2003, astro-ph/0305042.
- Whiting A.B. 2003, ApJ, 587, 186

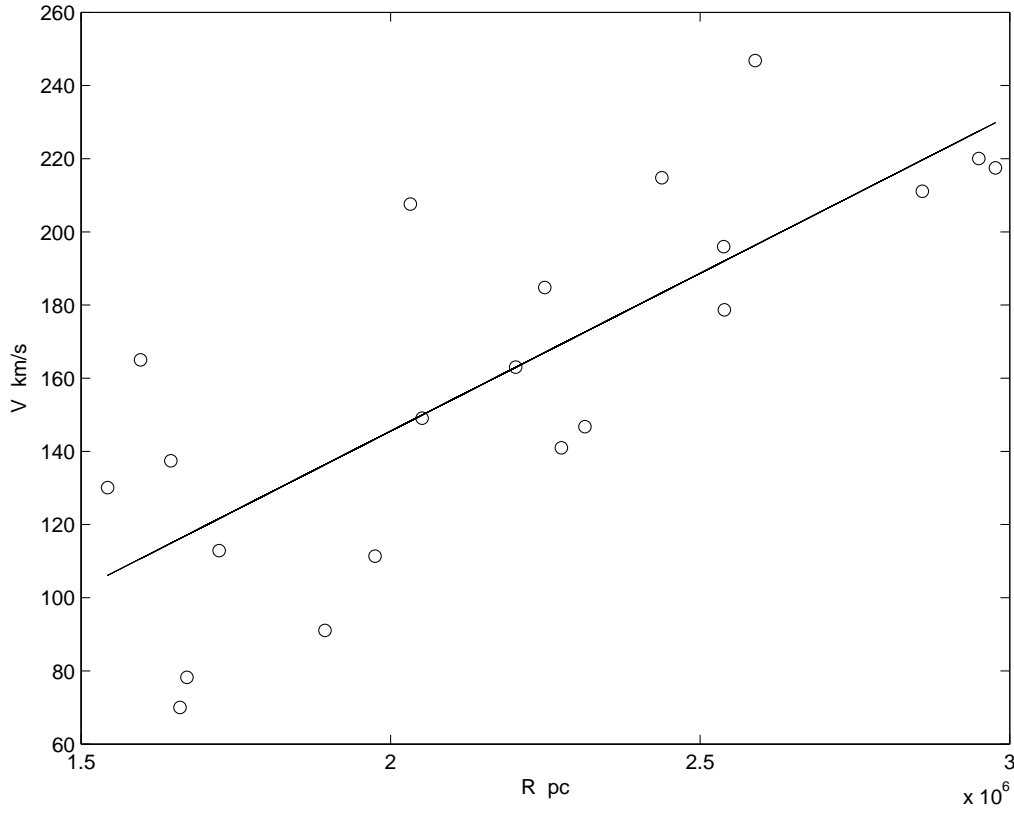


Fig. 1. Velocity-distance diagram for Sample 1.

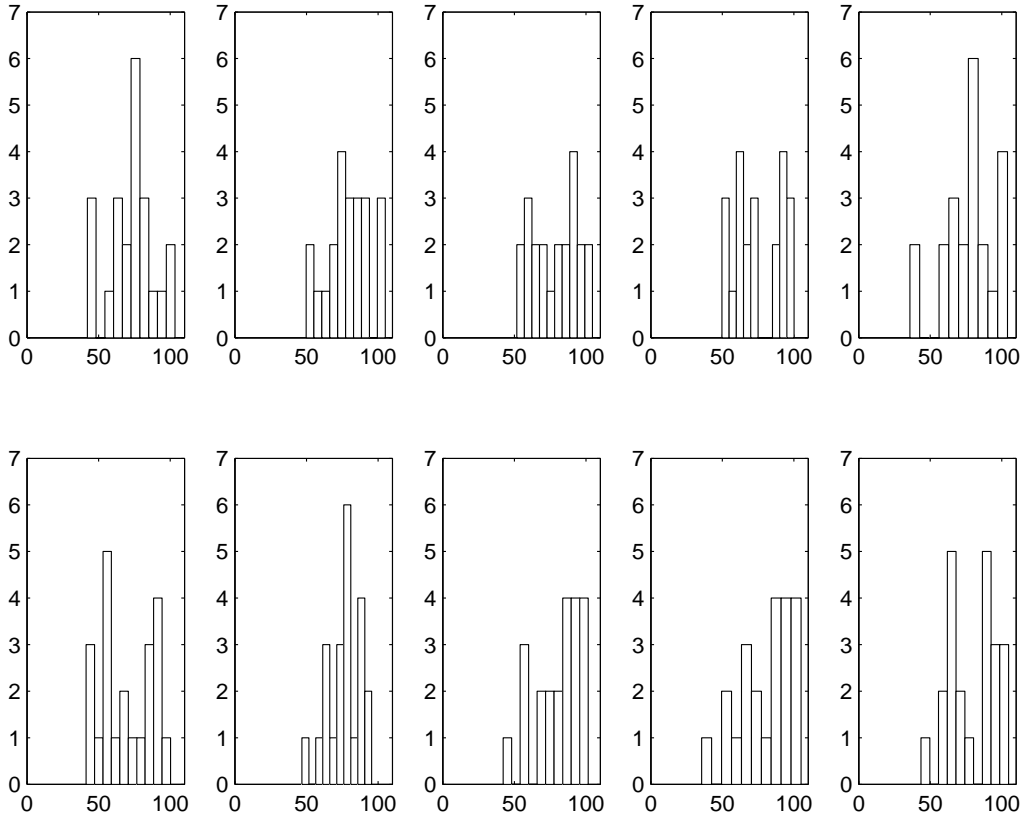


Fig. 2. Internal kinematic structure of simulation samples.

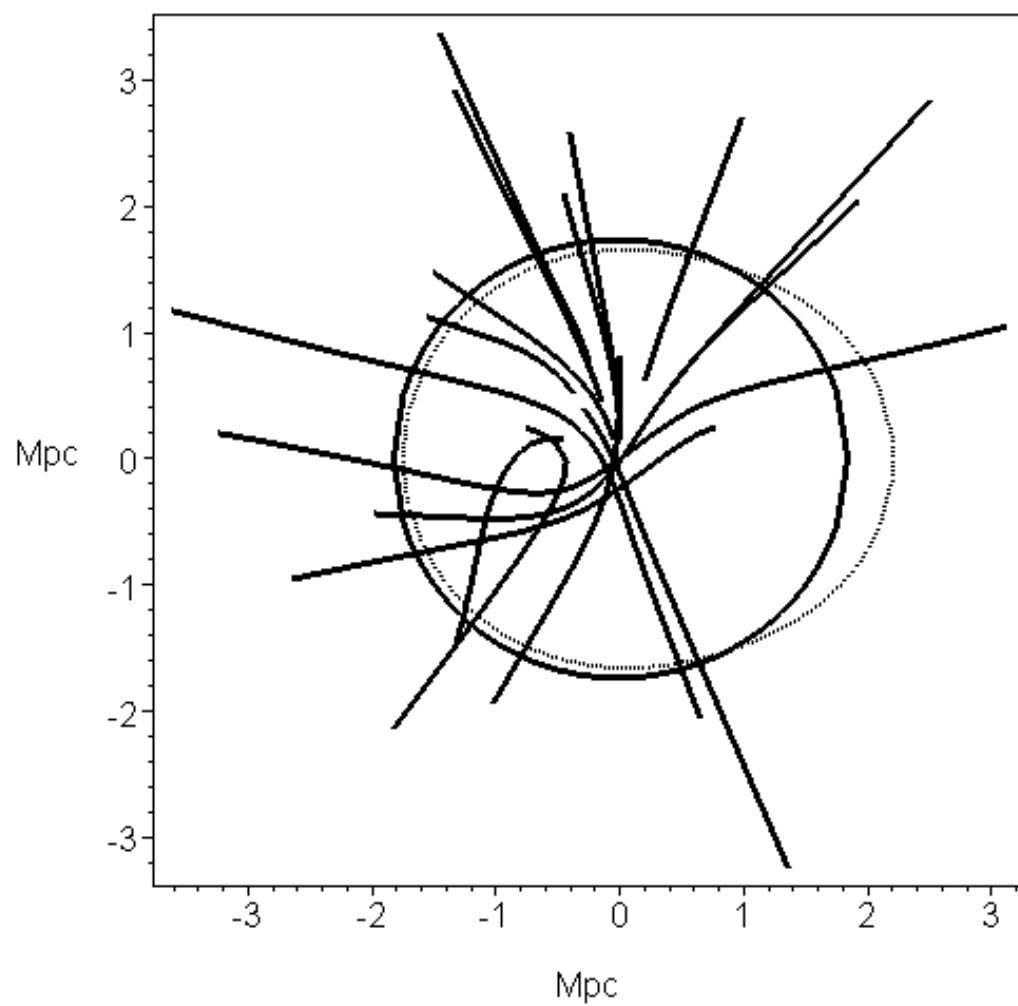


Fig. 3. Trajectories of Sample 1.

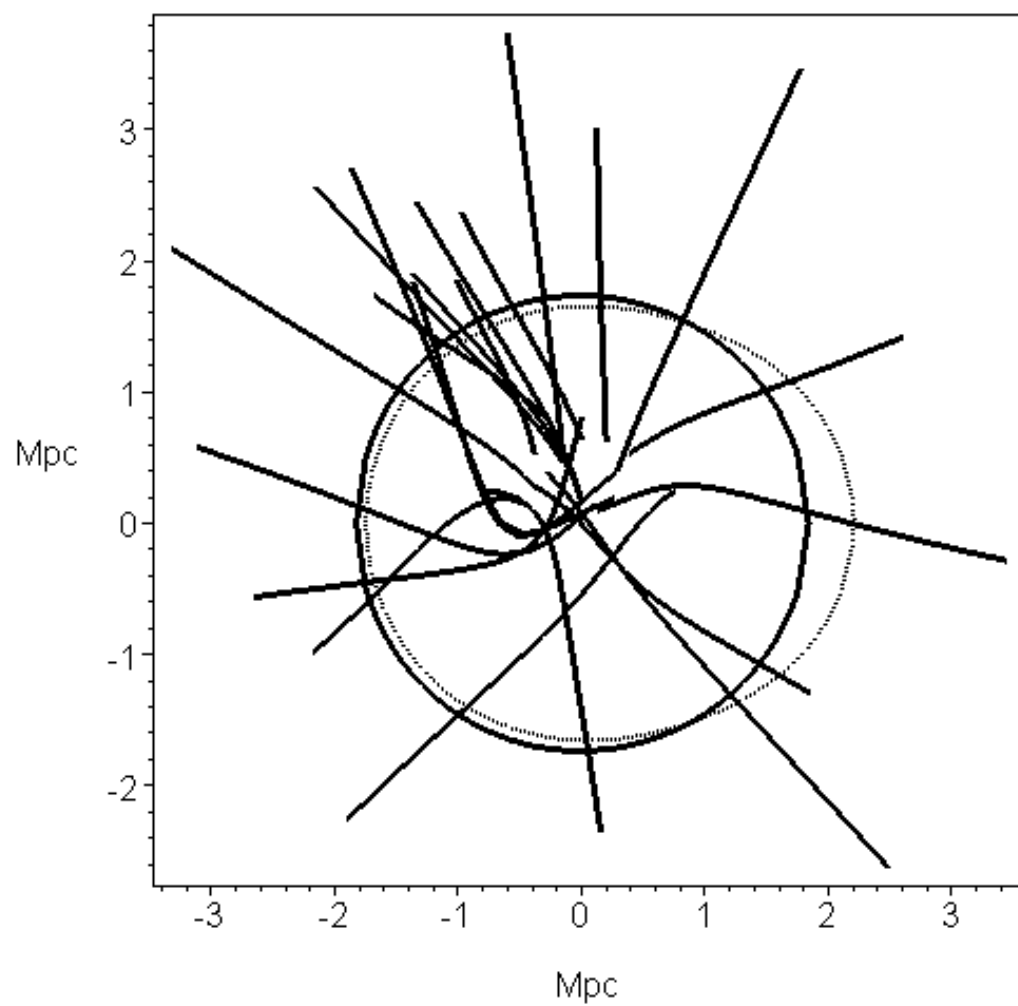


Fig. 4. Same for additional $\pm 50 \text{ km s}^{-1}$ initial transverse velocities.

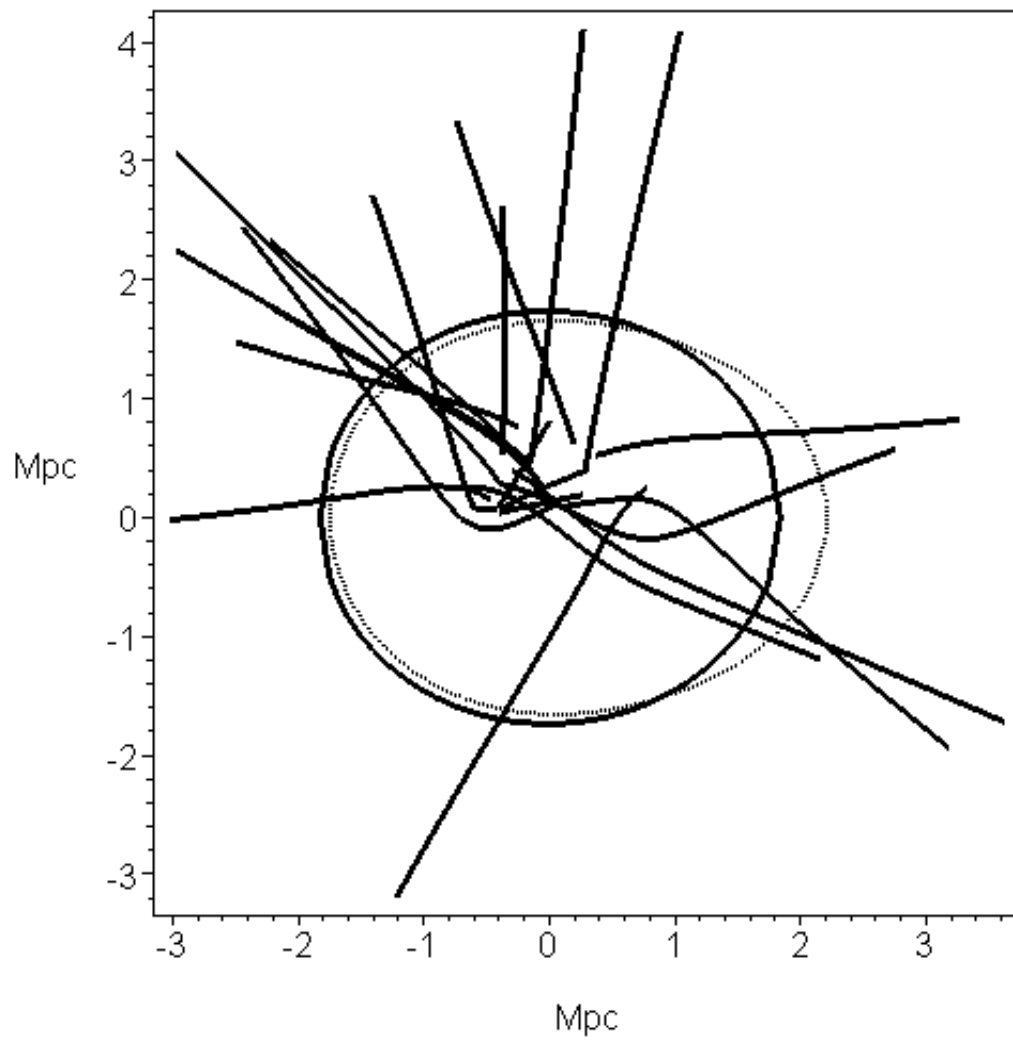


Fig. 5. Same for additional $\pm 100 \text{ km s}^{-1}$ initial transverse velocities.

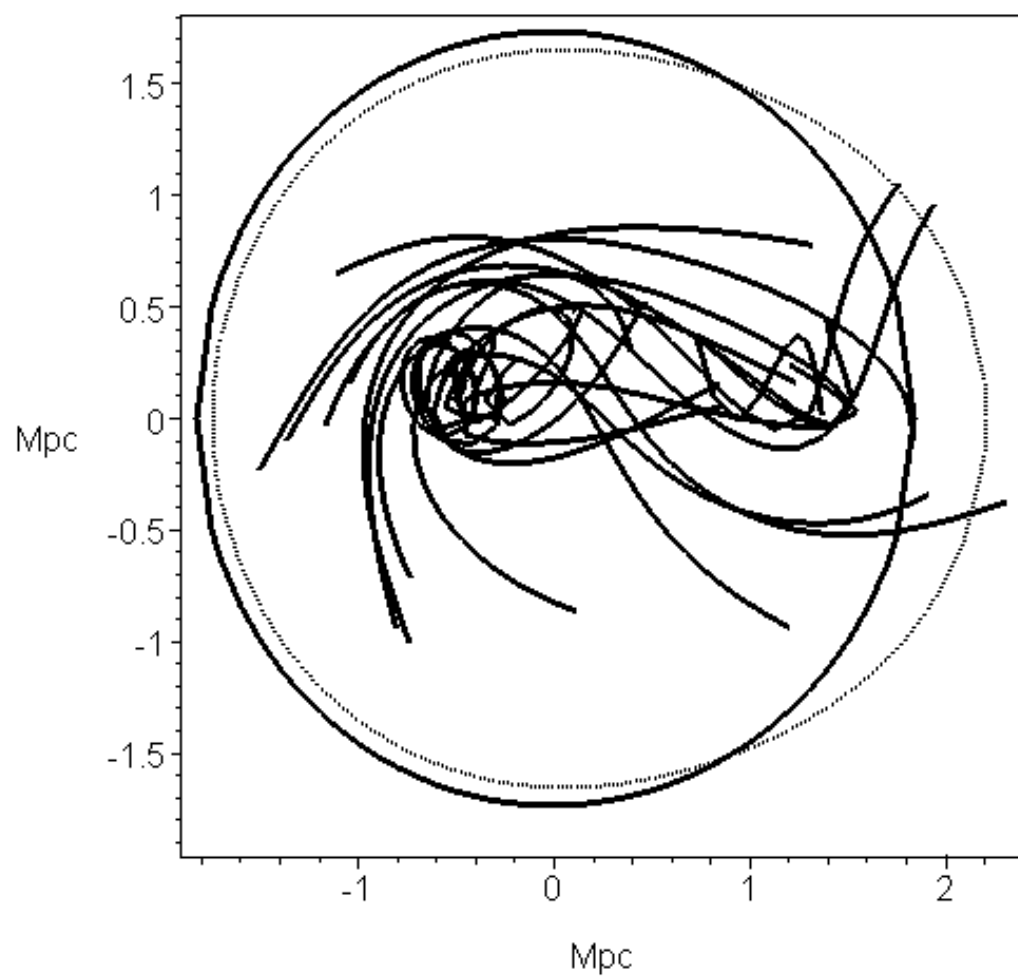


Fig. 6. Same for $\pm 100 \text{ km s}^{-1}$ initial transverse velocities and no radial velocities.